Line-shape theory and molecular dynamics in collision-induced light scattering

U. Balucani, V. Tognetti, and R. Vallauri
Laboratorio di Elettronica Quantistica del C.N.R., Via Panciatichi 56/30, Firenze, Italy
(Received 15 May 1978)

Molecular-dynamics studies in argon at 148 amagats are presented for gaining information on the dynamical properties responsible for the depolarized light scattering from simple fluids. The total and pair-correlation functions are computed within the simple dipole–induced-dipole model of polarizability anisotropy. The pair spectral shape is derived. These results are compared with a theoretical analysis based on a continued-fraction approach. The necessary frequency moments are calculated both in the low-density limit and taking into account first-order density corrections, and compared with the molecular-dynamics data. The agreement between the theoretical spectra and molecular-dynamics data shows the validity of the memory-function approach. The comparison with the real experimental results allows one to test the relevant physical contributions to the polarizability anisotropy.

I. INTRODUCTION

The depolarizing effect in the radiation scattered by a system of atoms (or spherical molecules) has been extensively studied in the past ten years both experimentally and theoretically.[1] The basic reason for the presence of depolarized scattered radiation is most easily seen in the low-density limit, where only binary collisions are important. Here the interatomic collisions induce a transient polarizability anisotropy in a pair of interacting atoms, producing an axially symmetric diatomic quasimolecule which accounts for the depolarizing effect. The duration of this polarizability anisotropy pulse is obviously connected with the frequency width of the observed depolarized spectrum.

The theoretical efforts for a better quantitative understanding of the phenomenon have proceeded along three main directions. The first one concerns the detailed mechanism of the induced polarizability anisotropy, which is exactly known only at large interatomic separations [dipole-induced-dipole (DID) limit]. The choice of a particular form for the polarizability anisotropy is reflected on the actual magnitude of the depolarized integrated intensity observed in the scattering process.

The second problem regards the shape of the scattered spectrum. Experimentally, nearly exponential line shapes are found. In a sense, this feature turns out to be less affected by the detailed form of the polarizability anisotropy or the interatomic potentials. Even so, it is difficult to arrive at a rigorous first-principle calculation of the line shape, particularly at arbitrary density. Often one must be content with the less ambitious task of comparing overall quantities, like the spectral slope and/or the first frequency moments with the experimental findings.

Finally, there is the interesting problem of the behavior of the spectra at higher densities (and possibly at various temperatures). Clearly in this case the simple binary collision model breaks down. The investigation of such features would be very useful for clarifying the dynamic properties of dense gases and liquids.

In this work we shall mainly deal with the line-shape problem of the spectrum due to pairs of interacting atoms at moderate density. In Sec. II the general expressions of the depolarized scattered intensity and of the frequency moments are summarized. The theoretical analysis used for evaluating the spectral shape is presented in Sec. III. For this purpose we shall use a memory-function approach which permits one to obtain in a consistent way the shape of the scattered spectrum if the first few frequency moments can be theoretically evaluated. A molecular dynamics experiment has been carried out in order to obtain both the "exact" time-correlation function and the spectral shape. Here the DID polarizability result has been used as a simple and convenient test of the validity of the theoretical approach. All these results are compared in Sec. IV, along with a discussion of the effects coming from finite-density corrections to the pair-distribution function. Finally, in Sec. V the line shapes obtained by the memory-function approach are compared both with the molecular-dynamics results and with the spectra observed in real experiments, thereby establishing the relevance of the various mechanisms for the polarizability in the different frequency regions of the spectra.

II. DEPOLARIZED SCATTERING CROSS SECTION

Assuming that the system polarizability can be written as a sum of pairwise contributions, the *total* depolarized scattering cross section turns out to be given by[1]:

$$I^{\vec{\epsilon}_i\vec{\epsilon}_f}(\omega)=\frac{1}{4}\left(\frac{\omega_i}{c}\right)^4\frac{1}{2\pi}\int_{-\infty}^{\infty}dt\,e^{-i\omega t}\times\left\langle\sum_{\substack{i,j\\ j\neq i}}\alpha_{ij}^{\vec{\epsilon}_i\vec{\epsilon}_f}(0)\sum_{\substack{k,l\\ l\neq k}}\alpha_{kl}^{\vec{\epsilon}_i\vec{\epsilon}_f}(t)\right\rangle . \tag{1}$$

Here ω is the frequency shift measured from the incident frequency ω_i ($\omega>0$ for the Stokes scattering). The polarization vectors of the incident and of the scattered fields are denoted by $\vec{\epsilon}_i$ and $\vec{\epsilon}_f$ respectively: for instance, in depolarized scattering $\vec{\epsilon}_i=\hat{Z}$, $\vec{\epsilon}_f=\hat{X}$. The quantity $\vec{\alpha}_{ij}$ is the polarizability tensor of atoms i and j, which depends on their mutual separation $\vec{R}_{ij}$. The summations run on the N atoms in the system, characterized by a volume V and a number density $\rho=N/V$.

In Eq. (1) one can separate out the different contributions due to pairs, triplets, and quadruplets of atoms.[1,2] In particular, the contribution due to atomic pairs is

$$I_2^{\vec{\epsilon}_i\vec{\epsilon}_f}(\omega)=\frac{1}{4}\left(\frac{\omega_i}{c}\right)^4\frac{1}{2\pi}\int_{-\infty}^{\infty}dt\,e^{-i\omega t}\times 2\sum_{\substack{i,j\\ j\neq i}}\langle\alpha_{ij}^{\vec{\epsilon}_i\vec{\epsilon}_f}(0)\alpha_{ij}^{\vec{\epsilon}_i\vec{\epsilon}_f}(t)\rangle . \tag{2}$$

In the low-density limit $I_2(\omega)$ accounts for most of the depolarized intensity.

Then we require a model for the polarizability tensor $\vec{\alpha}_{ij}$ of the pair i,j. Performing a multipole expansion, at first order one obtains the dipole-induced-dipole (DID) limit.

$$\alpha_{ij}^{\vec{\epsilon}_i\vec{\epsilon}_f}=2\alpha_0\delta_{\vec{\epsilon}_i,\vec{\epsilon}_f}+2\alpha_0^2T_{ij}^{\vec{\epsilon}_i\vec{\epsilon}_f}, \tag{3a}$$

where

$$T_{ij}^{\vec{\epsilon}_i\vec{\epsilon}_f}=\frac{1}{R_{ij}^3}\left((\vec{\epsilon}_i\cdot\vec{\epsilon}_f)-\frac{3}{R_{ij}^2}(\vec{\epsilon}_i\cdot\vec{R}_{ij})(\vec{\epsilon}_f\cdot\vec{R}_{ij})\right) \tag{3b}$$

and α_0 is the atomic polarizability. The result (3a) is exact, both classically and quantum mechanically, at relatively large distances R_{ij}.

The terms neglected in Eq. (3a) refers to various physical effects. First, higher-order multipole effects are of course present: even if classically at typical interatomic separations their effect is small, there is some quantum-theoretical[3] and experimental[4] evidence that they are not negligible. Moreover, there are also negative electronic overlap terms whose effect is still quantitatively unclear, in spite of the many empirical forms deduced for them from the experimental data.[5]

Even so, the large-separation result given by Eqs. (3a) and (3b) is on the whole a very good first approximation, simply because small distances R_{ij} are unlikely to be very effective due to the strong repulsive part of the interatomic potential. At least at low and moderate densities, the effect of the polarizability anisotropy other than that given by the DID mechanism is mainly seen on the integrated intensity of the spectra. As already noted, the spectral shape turns out to be comparatively less affected, particularly at low-frequency shifts (see also Sec. V). For all these reasons, in what follows we have explicitly considered only the DID polarizability, even if the theoretical approach can be straightforwardly used to include any other mechanism.

Instead of using Eq. (2), the dynamical processes due to scattering by atomic pairs can be investigated if the set of frequency moments

$$\overline{\omega^n}=\int_{-\infty}^{\infty}d\omega\,\omega^nI_2^{\vec{\epsilon}_i\vec{\epsilon}_f}(\omega),\quad n=0,1,2,\ldots \tag{4}$$

is known. In the classical limit, only even-frequency moments do not vanish since in this case $I_2(\omega)=I_2(-\omega)$. Quantum effects due to detailed balance factors must, however, be included if the classical results are compared with the real experimental spectra (see Sec. V).

The frequency moments $\overline{\omega^n}$ are calculated performing n time derivatives of the dynamic correlation function

$$\sum_{\substack{i,j\\ j\neq i}}\langle\alpha_{ij}(0)\alpha_{ij}(t)\rangle$$

and evaluating the result at $t=0$. Obviously, as n increases the procedure becomes more and more algebraically involved and tedious. It is therefore interesting to investigate whether it is possible to obtain an approximate spectral shape using the information contained in the first few frequency moments. In Sec. III we shall discuss a memory-function approach to this problem.[6]

For the spectrum due to the pairs, the zero-frequency moment (integrated intensity) is given by

$$\overline{\omega^0}=\frac{1}{2}\left(\frac{\omega_i}{c}\right)^4\rho^2V\frac{4\pi}{15}\int_0^{\infty}dR\,R^2\beta^2(R)g(R). \tag{5}$$

Here we have explicitly considered the case $\vec{\epsilon}_i\cdot\vec{\epsilon}_f=0$. In Eq. (5) $\beta(R)$ is the polarizability anisotropy associated to a couple of atoms separated by the distance R: in the DID limit one has $\beta(R)=6\alpha_0^2/R^3$. The quantity $g(R)$ is the density-dependent pair-distribution function. In the low-density limit it is simply given by $g_0(R)=\exp[-\varphi(R)/K_BT]$, where $\varphi(R)$ is the pair interatomic potential.

The expressions of $\overline{\omega^2}$ and $\overline{\omega^4}$, second and fourth moments of $I_2(\omega)$, are also known (see, e.g., the paper by Lallemand in Ref. 5). The sixth moment $\overline{\omega^6}$ can be calculated along the same lines; after a good deal of algebra we find[7]

$$\overline{\omega^6}=\frac{1}{2}\left(\frac{\omega_i}{c}\right)^4\rho^2V\frac{4\pi}{15}\left[\left(\frac{2K_BT}{m}\right)^3\int_0^\infty dR\left(7560\frac{\beta^2}{R^4}-8208\frac{\beta\beta'}{R^3}+2448\frac{\beta'^2}{R^2}+648\frac{\beta\beta''}{R^2}-792\frac{\beta'\beta''}{R}+216\frac{\beta\beta'''}{R}\right.\right.$$
$$\left.+234\beta''^2-144\beta'\beta'''+36R\beta''\beta'''+15R^2\beta'''^2\right)g(R)$$
$$+\frac{12}{m}\left(\frac{2K_BT}{m}\right)^2\int_0^\infty dR\,\varphi'\left(-72\frac{\beta^2}{R^3}+132\frac{\beta\beta'}{R^2}-24\frac{\beta\beta''}{R}-36\frac{\beta'^2}{R}\right.$$
$$\left.+6\beta'\beta''-6R\beta''^2-3R^2\beta''\beta'''\right)g(R)$$
$$-\frac{4}{m}\left(\frac{2K_BT}{m}\right)^2\int_0^\infty dR\,\varphi''\left(36\frac{\beta\beta'}{R}-24\beta'^2+6R\beta'\beta''+3R^2\beta''\beta'''\right)g(R)$$
$$+\frac{4}{m^2}\left(\frac{2K_BT}{m}\right)\int_0^\infty dR\,\varphi'^2\left(24\frac{\beta^2}{R^2}-72\frac{\beta\beta'}{R}+54\beta'^2+9R^2B''^2\right)g(R)$$
$$\left.+\frac{4}{m^2}\left(\frac{2K_BT}{m}\right)\int_0^\infty dR(\varphi''^2R^2\beta'^2+6\varphi'\varphi''R^2\beta'\beta'')g(R)\right]. \tag{6}$$

Here m is the atomic mass and the primes indicate derivatives with respect to R. As in the case of $\overline{\omega^4}$, an integration by parts simplifies somewhat Eq. (6), provided that $g(R)=\exp[-\varphi(R)/K_BT]$, clearly a bad approximation at moderate and high densities. The shape of the spectrum is essentially determined by the "normalized" frequency moments $\langle\omega^n\rangle\equiv\overline{\omega^n}/\overline{\omega^0}$.

III. MORI'S THEORY AND CORRELATION FUNCTION CALCULATION

We now deal with the calculation of time-correlation functions like $\langle MM(t)\rangle$, where M is the dynamical variable associated to the scattering. In the following we limit ourselves to the classical case. Let us define a "shape-correlation function"

$$f_0(t)=\langle M(0)M(t)\rangle/\langle M(0)M(0)\rangle \tag{7}$$

and its Laplace transform $\hat{f}_0(z)$. The frequency dependence of the spectrum is given by the Fourier transform of $f_0(t)$, i.e.,

$$f_0(\omega)=(1/\pi)\,\mathrm{Re}\hat{f}_0(z=i\omega). \tag{8}$$

Mori[8] has derived an exact equation of motion for $f_0(t)$ in terms of a memory function $f_1(t)$ which depends on higher-order time correlations. An equation of motion can also be written for $f_1(t)$ in terms of the corresponding memory function $f_2(t)$, and so on. Taking the Laplace transform of each equation of this infinite hierarchy, Mori arrives at the following continued-fraction representation for $\hat{f}_0(z)$:

$$\hat{f}_0(z)=[z+\Delta_1\hat{f}_1(z)]^{-1};$$
$$\hat{f}_j(z)=[z+\Delta_{j+1}\hat{f}_{j+1}(z)]^{-1}. \tag{9}$$

The quantities Δ_n are connected with the even-frequency moments $\langle\omega^{2n}\rangle$. In particular, the first three Δ_n are given by

$$\Delta_1=\langle\omega^2\rangle,\quad \Delta_2=\langle\omega^4\rangle/\Delta_1-\Delta_1,$$
$$\Delta_3=(1/\Delta_2)[\langle\omega^6\rangle/\Delta_1-(\Delta_1+\Delta_2)^2]. \tag{10}$$

The representation (9) is formally exact and reduces the dynamical problem to a static one. In practice, however, only the first few Δ_n can be theoretically evaluated and an approximate termination of the continued fraction is necessary. For spectral shapes without much structure it is sufficient to break the hierarchy by means of simple statistical approximations for $f_1(t)$ or, at most, $f_2(t)$. Defining

$$\hat{f}_j(z=i\omega)=a_j(\omega)-ib_j(\omega) \tag{11}$$

with

$$a_j(\omega)=\int_0^\infty f_j(t)\cos\omega t\,dt,$$
$$b_j(\omega)=\int_0^\infty f_j(t)\sin\omega t\,dt, \tag{12}$$

the spectral shape is found to be

$$f_0(\omega)=\frac{1}{\pi}\frac{\Delta_1a_1(\omega)}{[\omega-\Delta_1b_1(\omega)]^2+[\Delta_1a_1(\omega)]^2} \tag{13}$$

or

$$f_0(\omega)=\frac{1}{\pi}\frac{\Delta_1\Delta_2a_2(\omega)}{\{\omega[\omega-\Delta_2b_2(\omega)]-\Delta_1\}^2+\{\omega\Delta_2a_2(\omega)\}^2}, \tag{14}$$

according to whether the continued fraction is stopped at the first ($j=1$) or the second ($j=2$) stage, respectively.

Equations (13) and (14) are still exact, but require the knowledge of the quantities $f_1(t)$ or $f_2(t)$. Approximate forms can be deduced in particular cases, depending on the involved time scales and consequently on the frequency range of interest.[9] A Gaussian form for the memory function $f_j(t)$

$(j=1,2)$

$$f_j(t)=\exp(-\tfrac{1}{2}\Delta_{j+1}t^2) \tag{15}$$

has been found to give good results in several physical cases[10-12] for describing the overall features of the spectra. Indeed, such a memory function has the correct expansion in the $t\to 0$ limit and all the integrals $\int_0^\infty t^n f_j(t)\,dt$ exist. In the framework of the general memory-function theory of Ref. 8 the Gaussian termination (15) gives an approximate compromise behavior at all times: moreover, it has been exactly derived as a limiting case in a recent approach to the line-shape theory[13] which complements the previous memory-function theory. With the choice (15) the spectral shape functions given by Eq. (13) or (14) automatically conserve the first three and four even-frequency moments, respectively. The successive Δ are fixed by the Gaussian form of the memory function according to the relation

$$\Delta_{j+1+m}=(m+1)\Delta_{j+1}\,. \tag{16}$$

For a Gaussian $f_j(t)$ the quantities $a_j(\omega)$ and $b_j(\omega)$ are found to be

$$a_j(\omega)=(\pi/2\Delta_{j+1})^{1/2}\exp(-\omega^2/2\Delta_{j+1})\,,$$

$$b_j(\omega)=\frac{\exp(-\omega^2/2\Delta_{j+1})}{(\Delta_{j+1}/2)^{1/2}}\int_0^{\omega/(2\Delta_{j+1})^{1/2}}\exp(y^2)\,dy\,. \tag{17}$$

The corresponding spectral shape determined by Eq. (13) $(j=1)$ depends on the ratio Δ_2/Δ_1.[6,10] If the Gaussian termination is done at the second stage $[j=2$, Eq. (14)], the spectra show different features according to the ratios Δ_2/Δ_1 and Δ_3/Δ_2.[11] In any case, in collision-induced light scattering the values of the theoretical moments are such that only a single central peak at $\omega=0$ is found, as expected.

In the framework of the line-shape theory of Ref. 13 only two limiting cases were considered, which yielded either a Gaussian $f_j(t)$ or—in the long-time "Markoffian" limit—an exponential $f_j(t)$. A third intermediate limiting form is possible, and leads to

$$f_j(t)=\operatorname{sech}^2[(\tfrac{1}{2}\Delta_{j+1})^{1/2}t]\,. \tag{18}$$

The derivation is given in Appendix A. This memory function has the correct short-time expansion and an exponential long-time decay which is just the appropriate one if one neglects the processes which cause the very-long time tails.

In this case, different relationships are found among the successive Δ and in particular

$$\Delta_{j+2}=3\Delta_{j+1}\,. \tag{19}$$

The expressions of $a_j(\omega)$ and $b_j(\omega)$ are derived in Appendix A.

IV. MOLECULAR DYNAMICS EXPERIMENT

In this section we describe the computer simulation experiment and report the correlation functions pertinent to the problem.

A sample of $N=108$ atoms of argon is considered in a cubic box with an edge $L=30$ Å. This fixes the number density $\rho=148$ amagats. The atoms are assumed to interact through a Lennard-Jones (6-12) potential with parameters $\epsilon=119.8$ °K and $\sigma=3.405$ Å. The temperature of the system is chosen to be $T=294$ °K, which corresponds to a reduced temperature $T^*=K_BT/\epsilon=2.45$. A standard method of integration[14] of the Newton equations of motion is used along with periodic boundary conditions. The time step is $\Delta t=2\times10^{-14}$ sec. After a long run the system, starting from the solid fcc configuration with initial velocities assigned according to the desired temperature, reaches thermodynamic equilibrium. Then the dynamics of the N particles is followed during 24 000 more steps. In this time interval the averages of the time-correlation functions relevant for the problem are performed.

Two main correlation functions are evaluated. The first one is connected to the *total* depolarized light scattering spectrum,[15] namely,

$$C^{\vec\epsilon_i\vec\epsilon_f}(\tau)=\left\langle\sum_{\substack{i,j\\ j\neq i}}T_{ij}^{\vec\epsilon_i\vec\epsilon_f}(0)\sum_{\substack{k,l\\ l\neq k}}T_{kl}^{\vec\epsilon_i\vec\epsilon_f}(\tau)\right\rangle, \tag{20}$$

where now $\vec\epsilon_i\perp\vec\epsilon_f$.

The second one is the contribution to Eq. (20) due to *pairs* of atoms:

$$C_2^{\vec\epsilon_i\vec\epsilon_f}(\tau)=2\left\langle\sum_{\substack{i,j\\ j\neq i}}T_{ij}^{\vec\epsilon_i\vec\epsilon_f}(0)T_{ij}^{\vec\epsilon_i\vec\epsilon_f}(\tau)\right\rangle. \tag{21}$$

The maximum temporal delay at which the time-correlation functions are evaluated is $\tau_M=100\Delta t$, which corresponds to a time interval of 2×10^{-12} sec.

When averaged over the whole time interval of 24 000 steps the three correlation functions, corresponding to the choices of $\vec\epsilon_i$ and $\vec\epsilon_f$ along $\hat X,\hat Y,\hat Z$, turn out to have the same time behavior as expected, due to the fact that different components only stem out from a different scattering geometry.

In Fig. 1 the time-correlation functions, normalized to their $\tau=0$ values are reported. The dash-dot line represents the total correlation function while the dash-double-dot line is the pair contribution.

It is worthwhile noticing that in our previous ex-

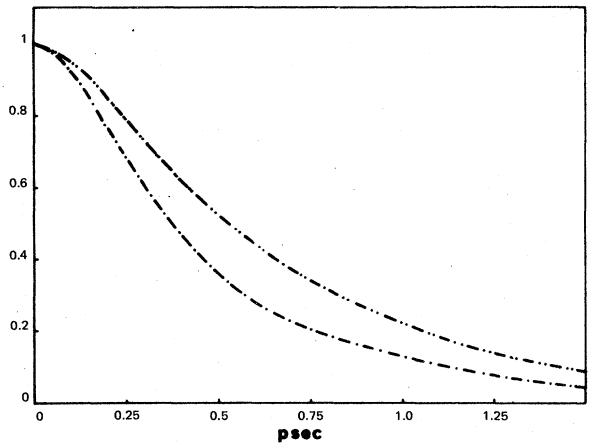

FIG. 1. Time-correlation functions for depolarized light scattering as given by the computer "experiment" in argon at room temperature and at 148 amagats. Dash-dot line, total correlation function; dash-double dot line, correlation function coming from atomic pairs. Both curves have been normalized to their respective values at $\tau = 0$.

periment 500 atoms of argon were used to derive the pair contribution in the same external conditions.[6] In that case the time average was performed over a shorter interval so that a larger spread of the three correlation functions was present at long time delays. Nevertheless, the average of the three components was substantially the same as the correlation function obtained in the present experiment. The lower accuracy achieved in the previous experiment was reflected in a larger oscillation of the frequency components of the spectrum in the region beyond 80 cm^{-1}. By the present results the frequency range can be extended to 170 cm^{-1} with higher accuracy.

We are now in a position to get information on a quantity which represents the contribution to the total depolarized intensity of the triplets and quadruplets. In fact if we write (dropping the labels $\vec{\epsilon}_i, \vec{\epsilon}_f$)

$$C(\tau)/C(0) = [C_2(\tau) + C_{3+4}(\tau)]/C(0), \tag{22}$$

we can extract $C_{3+4}(\tau)/C(0)$ by a simple subtraction, once $C(\tau)$, $C(0)$, and $C_2(\tau)$ are known. A comparison between the values of $C(0)$ and $C_2(0)$ obtained in the present molecular-dynamics experiment and a theoretical analysis will be made in Sec. V. In Fig. 2 we report the time behavior of the correlation functions as written in Eq. (22). At this stage we can only say that the long-lasting behavior of $C_{3+4}(\tau)$ and its negative contribution to the total integrated intensity is confirmed by real experiments[16] where both a fast decay of the three-body spectrum and a negative contribution to the total scattered intensity was observed.

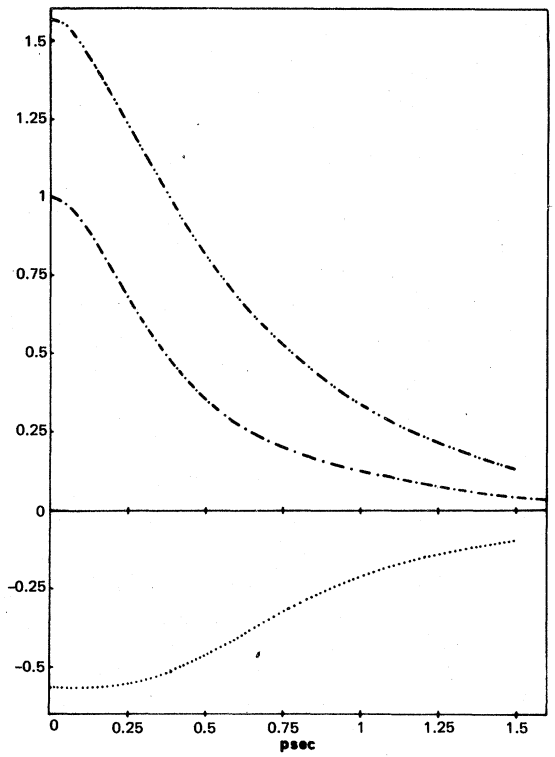

FIG. 2. Same as in Fig. 1, but with all curves normalized in such a way that $C(\tau = 0) = 1$. The time correlation function coming from the contribution of triplets and quadruplets of atoms (dotted line; see text) has also been drawn.

We now focus our attention on the pair contribution for which a detailed theoretical analysis is possible, as already shown. As will be shown in Sec. V, using the memory-function approach, that only the first three nonvanishing normalized moments of the pair spectrum are necessary. In order to perform the integrals appearing in the theoretical expressions of the moments the radial-distribution function $g(R)$ at the used density must be known. We have evaluated the "experimental" $g(R)$ in the interval $0.79 < x < 2.49$ ($x = R/\sigma$) counting for each atom the number of particles between x and $x + \Delta x$ ($\Delta x = 0.02$). An average over 24 000 steps is then performed. The function $g(R)$ so obtained is reported in Fig. 3 where the dash-dot line represents the zero-order approximation $g_0(R)$, the open circles are the "experimental" data, and the solid line is the distribution function when the first density correction to $g_0(R)$ is taken into account,[17] i.e.,

$$g(R_{12}) = g_0(R_{12})[1 + \rho g^{(1)}(R_{12})], \tag{23}$$

$$g^{(1)}(R_{12}) = \int d\vec{R}_3 \{\exp[-\varphi(R_{13})/K_B T] - 1\} \times \{\exp[-\varphi(R_{23})/K_B T] - 1\}, \tag{24}$$

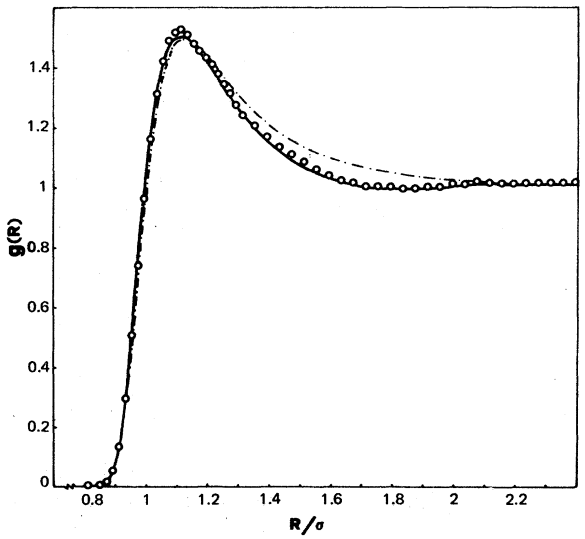

FIG. 3. Pair-distribution function for Lennard-Jones argon at room temperature and 148 amagats. Dash-dot line, zero-order result $g_0(R)$; solid line, theoretical $g(R)$ obtained taking into account first-order density corrections. The open circles are the pair-distribution function obtained in the computer experiment.

The result is quite satisfactory and stresses out the effects of finite density corrections. In Table I we report the value of the first moments evaluated performing the integrals with the "experimental" radial-distribution function. The integrals are corrected to account for the long-range contribution ($R > 2.49\sigma$) assuming that in this region the radial-distribution function is equal to unity. For comparison the values obtained in the zero- $[g(R) \equiv g_0(R)]$ and first-order approximation $\{g(R) \equiv g_0(R)[1+\rho g^{(1)}(R)]\}$ are also reported. As far as the moments are concerned the following information can be gained. Firstly, finite density corrections cause an increase of $\overline{\omega^n}$ larger and larger as n gets larger. Secondly, a small correction due to the contribution of a term proportional to ρ^2 in the radial-distribution function is apparent, and finally the sixth moment cannot be evaluated by this method since detailed information on the radial-distributuion function below $x = 0.79$ is necessary. As is apparent from Eq. (6) the integrals in $\overline{\omega^6}$ involve higher-order derivatives of the potential energy, which are relevant just in the region below $x = 0.79$ where the counts in the computer experiment are too small to give any reliable result.

Two alternative methods for the evaluation of the moments from the "experimental" results are possible. The first one is to expand the correlation function as a power series of time and evaluate the coefficients of the three terms by a fitting procedure. By the second method one simply evaluates the integrals (4) using the "experimental" spectrum $I_2(\omega)$ deduced from the correlation function. As a matter of fact these two methods turn out to give unreliable results even for the fourth moment. Namely, a precise evaluation of the time coefficients needs the values of the correlation function at times such that terms higher than the required ones are already important: unfortunately, the accuracy of the computed $C(\tau)$ does not allow this polynomial fitting at such high orders. On the other hand, the second method requires knowledge of the spectrum in a frequency region where a substantial oscillation already appears in the experimental spectra.

V. RESULTS AND DISCUSSION

In this section we compare the molecular-dynamics data with the theoretical results. The first quantities of interest are the integrated intensities $C(0)$ and $C_2(0)$. It is convenient to introduce the dimensionless quantities[2]

$$S \equiv (\sigma^6/N)C(0), \quad 2S_2 \equiv (\sigma^6/N)C_2(0). \tag{25}$$

In our molecular-dynamics experiment ($\rho = 148$ amagats) S and $2S_2$ turn out to be 0.7133 and 1.1167, respectively. The contribution of the pairs can be easily deduced from Eq. (5): in the zero-order approximation for $g(R)$ we obtain $2S_2 = 1.1222$. As is apparent from the $\overline{\omega^0}$ values re-

TABLE I. The DID frequency moments of the pair spectrum together with the related quantities Δ_n. The numbers refer to Lennard-Jones argon at a reduced temperature $T^* = 2.45$ and at a density of 148 amagats. In these conditions the frequency $\Omega_0 \equiv (2K_B T/m\sigma^2)^{1/2}$ turns out to be 5.432 cm^{-1}. (a) Refers to the low-density g_0 limit, (b) to the theoretical $g(R)$ with first-order density corrections, (c) to the experimental $g(R)$. A factor $\frac{12}{15}\pi \times (\omega_i/c)^4\rho^2 V\alpha_0^2/\sigma^3$ is present in all moments $\overline{\omega^n}$ and has been left out.

	$\overline{\omega^0}$	$\overline{\omega^2}/\Omega_0^2$	$\overline{\omega^4}/\Omega_0^4$	$\overline{\omega^6}/\Omega_0^6$	Δ_1/Ω_0^2	Δ_2/Ω_0^2	Δ_3/Ω_0^2
(a)	0.4752	4.847	619.2	4.36×10^5	10.2	117.55	627
(b)	0.4746	4.895	654.3	...	10.315	123.35	...
(c)	0.4783	4.958	697.2	...	10.36	130	...

ported in Table I, practically the same result is obtained even taking into account the first density correction to $g_0(R)$.

The total depolarized intensity is the sum of $2S_2$ and analogous contributions $4S_3$ and S_4 coming from triplets and quadruplets of atoms. The theoretical expression of the triplet contribution is known[1] and can be exactly evaluated in the low-density limit where the three-body distribution function factorizes in a product of three pair functions $g_0(R)$. In our case, we find $4S_3 = -0.5418$ so that the theoretical contribution due to the pairs and the triplets turns out to be $2S_2 + 4S_3 = 0.5804$. This is to be compared with the "experimental" total value of $S(0) = 0.7133$, giving a clear evidence that the quadruplet contribution S_4 is positive. Theoretically, the computation of the multiple integrals involved in the expression of S_4 is very difficult even in the low-density limit.

Let us now discuss in detail the shape of the spectrum due to the pairs. The "experimental" spectrum is obtained by Fourier transforming the molecular-dynamics data for the time-correlation function $C_2(\tau)$ of Eq. (21). This has been done numerically by a fast-Fourier-transform method. The result is plotted in Fig. 4 (open circles) up to a frequency $\omega = 170$ cm^{-1} (note the logarithmic vertical scale). It is apparent that the purely DID mechanism for the polarizability leads to a spectral shape which is neither a single exponential nor a sum of two exponentials. This feature has already been noted in theoretical evaluations of the line shape at low densities[18] as well as in real experiments.[4]

In Fig. 4 the spectral shapes obtained with two possible terminations at the *first order* of the continued fraction have also been plotted. They correspond to the Gaussian and $\mathrm{sech}^2 x$ approximations for $f_1(t)$ discussed in Sec. III. Here in order to make the most direct comparison with the molecular-dynamics data, the quantities Δ_1 and Δ_2 have been deduced using the "experimental" values of $\overline{\omega^0}$, $\overline{\omega^2}$, $\overline{\omega^4}$ reported in Table I. In this figure, as well as in the following ones, both the "experimental" and the theoretical curves have been normalized to the same integrated intensity. From Fig. 4 one sees that some overall features of the spectrum are already reproduced even in this first-order termination. The deviations beyond $\omega \sim 60$ cm^{-1} can be easily explained. Whatever termination is used at first order, Δ_3 (and consequently the sixth moment) is automatically fixed: for the Gaussian and $\mathrm{sech}^2 x$ one would find $\overline{\omega^6} = (2.63 \times 10^5)\Omega_0^6$ and $(3.5 \times 10^5)\Omega_0^6$, respectively. The corresponding values of Δ_3 are $260\Omega_0^2$ and $390\Omega_0^2$. Even if it is difficult to establish the value of $\overline{\omega^6}$ using the "experimental" $g(R)$ in Eq. (6), these predicted first-order values are undoubtedly too low. For instance, if we use the low-density distribution function $g_0(R)$ the quantity $\overline{\omega^6}$ turns out to be $(4.36 \times 10^5)\Omega_0^6$ and consequently $\Delta_3 = 627\Omega_0^2$. These drawbacks of the first-order terminations have already been pointed out in the Gaussian case.[6]

In Fig. 5 we have plotted the spectral shapes ob-

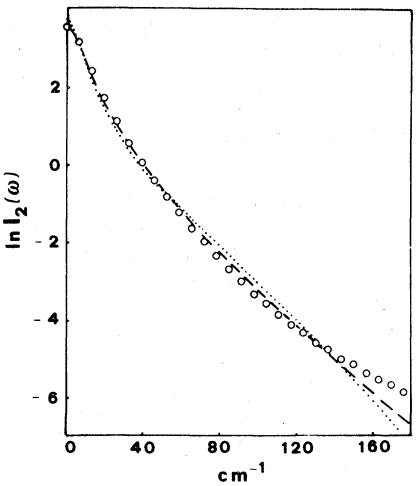

FIG. 4. Spectral shape for the depolarized spectrum due to the pairs. The open circles refer to the molecular-dynamics data. The dashed and the dotted lines are the result of a first-order memory-function theory with $\mathrm{sech}^2 x$ and Gaussian terminations, respectively. The necessary frequency moments have been evaluated by means of the "experimental" $g(R)$.

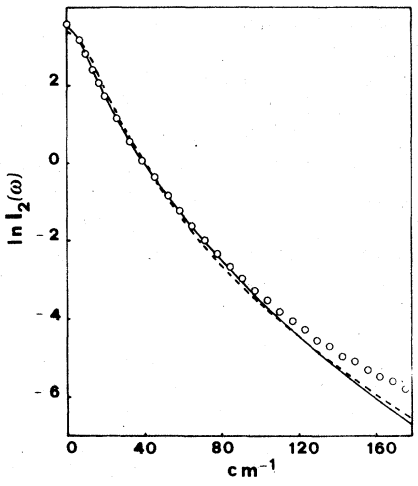

FIG. 5. Same as in Fig. 4, but with the theoretical curves obtained by means of a second-order memory-function approach. The full and the dashed lines refer to a $\mathrm{sech}^2 x$ and to a Gaussian termination, respectively. The necessary frequency moments have been evaluated using the low-density limit for the pair-distribution function.

tained using the same terminations at the *second order* of the continued fraction. Since the value of $\overline{\omega^6}$ can be exactly determined only in the $g_0(R)$ limit, to be consistent we have used the quantities Δ_1, Δ_2, Δ_3 in the same low-density approximation. Even so an improved agreement is evident up to frequencies $\omega \sim 100$ cm^{-1} for both types of terminations. Therefore, as far as the spectral shape is concerned the theory at the second stage gives good results for most of the spectrum without requiring a detailed knowledge of high-order memory functions.

A more stringent test of the validity of the various terminations is the comparison of the corresponding time-correlation functions as shown in Fig. 6(a) and 6(b). It is apparent from Fig. 6(a), which is obtained in the g_0 limit, that the sech^2x termination gives a better agreement with the molecular-dynamics data. Obviously, the agreement can be improved using the quantities Δ_1 and Δ_2 deduced from the "experimental" $g(R)$ and letting Δ_3 as an adjustable parameter for a best fitting of the sech^2x form. The result of this procedure [shown in Fig. 6(b)] gives $\Delta_3 = 630\Omega_0^2$ which corresponds to $\overline{\omega^6} = (5 \times 10^5)\Omega_0^6$. If the fitting were performed on the Gaussian, we would obtain $\Delta_3 = 500\Omega_0^2$ and a corresponding value of the sixth moment $[(4.2 \times 10^5)\Omega_0^6]$, which is unreasonably low on the basis of the finite-density corrections presented in Table I. Again, also in this case the spectral shapes (Fig. 7) for both terminations appear to be in excellent agreement with the molecular-dynamics data.

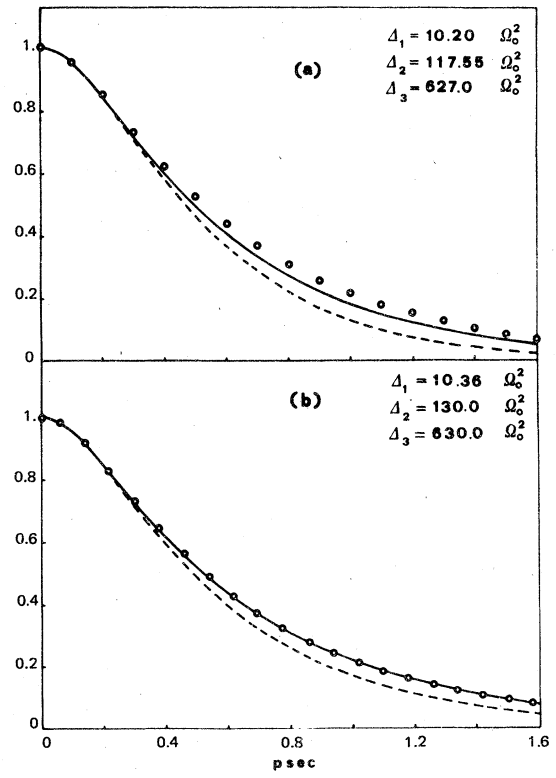

FIG. 6. Time correlation function $C_2(\tau)/C_2(0)$ due to the pairs. The open circles are the molecular-dynamics data already reported in Fig. 1. The full and the dashed lines refer to a sech^2x and to Gaussian second-order terminations, respectively. In (a) the frequency moments correspond to the g_0 limit; in (b) they have been evaluated as described in the text.

Finally, it is interesting to compare the spectra obtained with the DID polarizability with the shape observed in real experiments for the "two-body" intensity. In practice, the latter is obtained extracting from the total depolarized spectrum the contribution proportional to the square of the density: this component is directly comparable with the pair spectrum in the lowest-order approximation for $g(R)$. In a recent work[4] the two-body part of the room-temperature spectrum of argon has been reported up to 250 cm^{-1}. In our units the measured normalized second and fourth moments turn out to be $\langle\omega^2\rangle = \Delta_1 = 8.14\Omega_0^2$, $\langle\omega^4\rangle = 760\Omega_0^4$ and consequently $\Delta_2 = 85.2\Omega_0^2$. From Fig. 8 one sees that the experimental spectrum is satisfactorily reproduced by a second-order sech^2x termination if a $\Delta_3 \sim 380\Omega_0^2$ is chosen as a fitting parameter. The corresponding value of $\langle\omega^6\rangle$ turns out to be $(3.34 \times 10^5)\Omega_0^6$.

A comparison between the real experiment and the molecular-dynamics data allows us to establish in a direct way the presence and the relevance of mechanisms for the polarizability anisotropy other than the DID one. Indeed from Fig. 8 it appears that the DID mechanism accounts with good

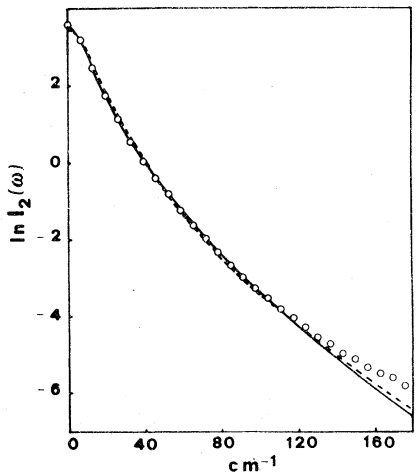

FIG. 7. Same as in Fig. 5, but with the frequency moments as in Fig. 6 (b).

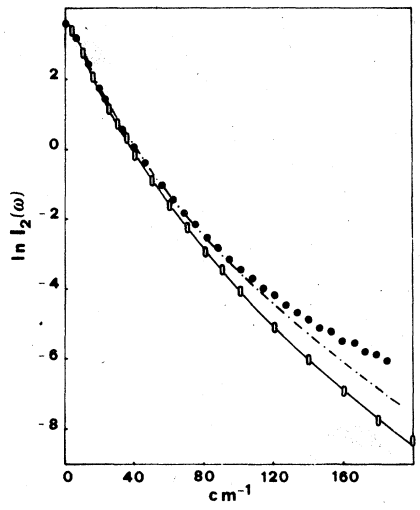

FIG. 8. Comparison between the pair spectrum as given by the molecular-dynamics simulation (black dots) and the two-body experimental spectrum in real argon at room temperature (open ovals). For the latter data the effect of the detailed balance factor has been subtracted out. The full line is the second-order result based on the experimental frequency moments reported in Ref. 4. The dot-dashed line is the second-order result with the DID moments in the g_0 limit. Both these curves correspond to a $\mathrm{sech}^2 x$ termination.

accuracy for the low-frequency behavior of the two-body spectrum. As a matter of fact, the long-time behavior of the correlation function is mainly determined by the long-range part of the polarizability which is dominated by a purely DID mechanism. Beyond 80 cm^{-1} the evident discrepancy between the molecular-dynamics data and the experimental points is quite interesting. The finite density $g(R)$ increases the effective contribution of the short distances as is apparent from Fig. 3. One may think that this is the cause of the deviation with respect to the experimental two-body spectrum, which by definition corresponds to the low-density limit. However, the comparison between the experimental data and the DID spectrum obtained by the memory-function approach in the $g_0(R)$ limit shows (Fig. 8) that finite density corrections are not sufficient to account for this discrepancy. This is clear evidence that a short-range contribution to the polarizability anisotropy is not negligible. To our knowledge the only theoretical attempt to derive in argon an electronic overlap contribution is due to Gelbart *et al.*[19,20] However, their expression of the polarizability leads to frequency moments still in disagreement with the experimental values of Ref. 4: the frequency moments theoretically derived in Ref. 20 lead to $\Delta_1 = 8.45\Omega_0^2$ and $\Delta_2 = 52.4\Omega_0^2$. Moreover, the corresponding ratio Δ_2/Δ_1 is 6.20 and leads to a nearly exponential shape in contrast with the experimental two-body spectrum.

VI. CONCLUSION

In this work we have shown that a theoretical analysis based on a memory-function approach combined with molecular-dynamics calculations is a useful method for gaining information on those dynamical properties responsible for the depolarized scattering of light from simple fluids. Moreover, the comparison with the real experimental data allows one to test the relevant physical contributions to the polarizability anisotropy. We have focused our attention on the classical dipolar contribution and demonstrated the validity of the memory-function approach in this well-defined physical situation. In this way as soon as a more detailed theoretical knowledge of the pair polarizability is available, the use of the methods discussed here permits one to verify the validity of the predictions by a straightforward comparison with the experimental spectral shapes.

ACKNOWLEDGMENTS

We wish to acknowledge fruitful and stimulating discussions with Dr. F. Barocchi, Dr. M. Zoppi and Dr. G. Jacucci. One of us (R.V.) thanks Professor K. Singer for his most valuable help at the beginning of this work, during the stay at Royal Holloway College of the University of London as British Council Student.

APPENDIX A

In a recent paper Tokuyama and Mori[13] present a different approach in order to obtain a new equation for the jth-order memory function. In this framework the equation of motion for $f_j(t)$ assumes the following exact form:

$$\frac{d}{dt} f_j(t) = -\Omega_j(t) f_j(t) , \tag{A1}$$

where

$$\Omega_j(t) = \Delta_{j+1} \int_0^t \psi_j(\tau)\, d\tau \tag{A2}$$

is a generalized frequency. The frequency modulation function $\psi_j(t)$ can be derived from the equation of motion of the variables of the system by means of a projection-operator method. A relationship between ψ_j and f_{j+1} has been obtained and the two theories can complement each other giving the possibility of a unified point of view. Integrating Eq. (A1), one obtains

$$f_j(t) = \exp\left(-\Delta_{j+1} \int_0^t (t-\tau)\psi_j(\tau)\, d\tau \right). \tag{A3}$$

This expression has been derived also in the stochastic theory of line shape[21] and turns out to be powerful for simple special cases of $\psi_j(t)$. If the frequency modulation $\psi_j(t)$ has the same time decay as $f_j(t)$, the latter can be inserted in the right-hand side of Eq. (A3) which becomes

$$f_j(t) = \exp\left(-\Delta_{j+1}\int_0^t (t-\tau) f_j(\tau)\, d\tau\right). \tag{A4}$$

The solution of (A4) can be obtained by differentiating twice, and turns out to be

$$f_j(t) = \operatorname{sech}^2[(\tfrac{1}{2}\Delta_{j+1})^{1/2} t]. \tag{A5}$$

From Eq. (A5) the expressions of $a_j(\omega)$ and $b_j(\omega)$ can be found. The expression of $a_j(\omega)$ is simply given by

$$a_j(\omega) = \int_0^\infty \operatorname{sech}^2[(\tfrac{1}{2}\Delta_{j+1})^{1/2} t]\cos \omega t\, dt = \frac{\pi\omega}{\Delta_{j+1}\sinh[\pi\omega/(2\Delta_{j+1})^{1/2}]}. \tag{A6}$$

For $b_j(\omega)$ the integral

$$b_j(\omega) = \int_0^\infty \operatorname{sech}^2[(\tfrac{1}{2}\Delta_{j+1})^{1/2} t]\sin \omega t\, dt \tag{A7}$$

can be expressed by means of a series expanding $\sin\omega t$ and integrating term by term, i.e.,

$$b_j(\omega) = 2(\omega/\Delta_{j+1})\ln 2 + \sum_{k=2}^{\infty} (-1)^{k-1}\left(\frac{2}{\Delta_{j+1}}\right)^k \frac{4^{k-1}-1}{4^{2(k-1)}}\,\zeta(2k-1)\,\omega^{2k-1}, \tag{A8}$$

where $\zeta(x)$ is the Riemann function. Within an accuracy of 1% only few terms are sufficient until $\omega \sim (\Delta_{j+1})^{1/2}$ and the number of these terms remains reasonable until $\omega \sim (2\Delta_{j+1})^{1/2}$. Beyond this frequency value the Gaussian $b_j(\omega)$ of Eq. (17) turns out to give a good approximate expression for $b_j(\omega)$ also for this $\operatorname{sech}^2 x$ termination.

[1] See the review paper by W. M. Gelbart, Adv. Chem. Phys. 26, 1 (1974), and references therein.

[2] B. J. Alder, J. J. Weis, and H. L. Strauss, Phys. Rev. A 7, 281 (1973).

[3] P. H. Certain and P. J. Fortune, J. Chem. Phys. 55, 5818 (1971).

[4] F. Barocchi and M. Zoppi, Phys. Lett. A 66, 99 (1978).

[5] H. B. Levine and G. Birnbaum, J. Chem. Phys. 55, 2914 (1971); P. Lallemand, C. R. Acad. Sci. (Paris) 273, 89 (1971); J. P. McTague, W. D. Ellenson, and L. H. Hall, J. Phys. (Paris) 33-C1, 241 (1972).

[6] Preliminary results of the application of these methods to collision light scattering have been reported in the U. Balucani, V. Tognetti, and R. Vallauri, Phys. Lett. A 64, 387 (1978).

[7] $\overline{\omega^6}$ has also been evaluated by a different method but with the same result by M. Zoppi (private communication).

[8] H. Mori, Prog. Theor. Phys. 33, 423 (1965); 34, 399 (1965).

[9] For a discussion about the limiting cases see, e.g., U. Balucani and V. Tognetti, Phys. Rev. B 16, 271 (1977).

[10] K. Tomita and H. Tomita, Prog. Theor. Phys. 45, 1407 (1971).

[11] K. Tomita and H. Mashiyama, Prog. Theor. Phys. 51, 1312 (1974).

[12] See J. R. D. Copley and S. W. Lovesey, Rep. Prog. Phys. 38, 461 (1975).

[13] M. Tokuyama and H. Mori, Prog. Theor. Phys. 55, 411 (1976).

[14] L. Verlet, Phys. Rev. 165, 21 (1968).

[15] Molecular-dynamics experiments which measure this correlation function have been also reported by B. J. Alder, H. L. Strauss, and J. J. Weis, J. Chem. Phys. 59, 1002 (1973).

[16] P. Lallemand, J. Phys. (Paris) 32, 119 (1971); J. P. McTague, W. D. Ellenson, and L. H. Hall, J. Phys. (Paris) 33-C1, 241 (1972); F. Barocchi and J. P. McTague, Phys. Lett. A 53, 488 (1975).

[17] D. Henderson, Mol. Phys. 10, 73 (1966).

[18] J. I. Gersten, Phys. Rev. A 4, 98 (1971).

[19] D. F. Heller, R. A. Harris, and W. M. Gelbart, J. Chem. Phys. 62, 1947 (1975).

[20] D. W. Oxtoby and W. M. Gelbart, Mol. Phys. 29, 1569 (1975).

[21] R. Kubo, "A Stochastic Theory of Line-shape and Relaxation," in *Fluctuation, Relaxation and Resonance in Magnetic Systems*, edited by D. ter Haar (Oliver and Boyd, London, 1962).